Bonding and Energy Dissipation in a Nanohook Assembly

Savas Berber, Young-Kyun Kwon,* and David Tománek†
Department of Physics and Astronomy, Michigan State University, East Lansing, Michigan 48824-2320
(Dated: May 17, 2003)

Combining total energy and molecular dynamics calculations, we explore the suitability of nanotube-based hooks for bonding. Our results indicate that a large force of 3.0 nN is required to disengage two hooks, which are formed by the insertion of pentagon-heptagon pairs in a $(7,0)$ carbon nanotube. Nanohooks based on various nanotubes are resilient and keep their structural integrity during the opening process. Arrays of hooks, which are permanently anchored in solid surfaces, are a nanoscale counterpart of velcro fasteners, forming tough bonds with a capability of self-repair.

PACS numbers: 81.07.De, 61.48.+c, 68.70.+w, 81.05.Zx

Carbon nanotubes [1], consisting of graphite layers rolled up to seamless, nanometer-wide cylinders, are now considered important building blocks for nanotechnology [2]. Their extraordinary mechanical properties, including high stiffness [3–5] and axial strength [6, 7], are related to the unparalleled tensile strength of graphite [8]. In single-wall nanotubes [9, 10], substitution of hexagons by pentagon-heptagon pairs is known to cause a permanent bend in the tube and to change its chirality [11]. The morphology of a nanotube deformed to a hook is illustrated schematically in Fig. 1(a). A High-Resolution Trasmission Electron Micrograph (HRTEM) of this system [12] is reproduced in Fig. 1(b), and a Scanning Electron Micrograph (SEM) of nanohooks [13] is shown in Fig. 1(c). So far, studies of nanotubes containing pentagon-heptagon pairs have concentrated on their intriguing electronic properties [14].

Here we explore the suitability of nanotubes, permanently deformed to hooks or other non-cylindrical structures, to effectuate bonding between solid surfaces [15], as a nanometer-scale counterpart of velcro. We study the physical properties, including mechanical strength and resilience, of a micro-fastening system consisting of solid surfaces covered with nano-hooks, illustrated in Fig. 2(a) and Fig. 1(c), which we call 'nanovelcro'. By studying the atomic-scale processes during closure and opening, we show that a nanovelcro junction should be ductile rather than brittle, and exhibit large toughness. We find that nanovelcro offers significant advantages over conventional adhesives and welding, including thermal stability to 4,000 K, and a self-repair mechanism under local shear. With a large density of hooks per area, strong bonding can be achieved in parallel to mechanically decoupling the connected parts.

To determine the physical behavior of the nanovelcro micro-fastening system, we combine total energy and structure optimization calculations with molecular dynamics simulations. In order to describe realistically a possible $sp^2 \rightarrow sp^3$ rehybridization during the opening and closing of nanovelcro bonds, we use an electronic Hamiltonian that had been applied successfully to describe the formation of peapods [16], multi-wall nanotubes [17], the dynamics of the "bucky-shuttle" [18], and the melting of fullerenes [19]. Total energies and forces are compared to those based on the Tersoff potential [20] for strained structures that maintain sp^2 bonding. When modelling the dynamical processes during opening and closure of the hook assembly in Fig. 2(a), we subject the grey-shaded rigid anchor sections to either a constant force

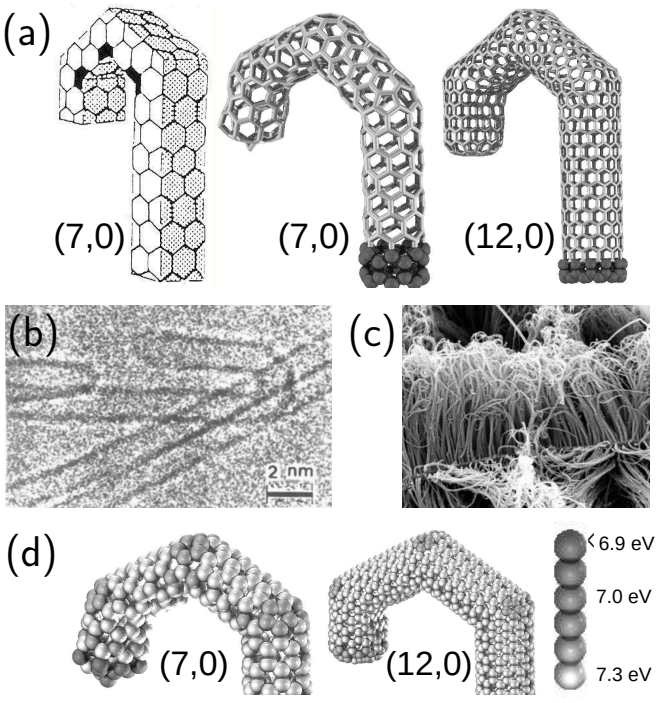

FIG. 1: Structure of a nanotube-based hook. (a) Schematic view of a hook, formed by inserting pentagon-heptagon pairs in an all-hexagon tubular structure, and the equilibrium structure of hooks based on a (7,0) and a (12,0) nanotube. (b) Transmission Electron Micrograph of a nanotube-based hook, published in Ref. 12. (c) Scanning Electron Micrograph of an array of nanohooks grown on a surface [13]. (d) Atomic binding energies in (7,0) and (12,0) nanohooks. The grey scale coding reflects the energy scale on the right.

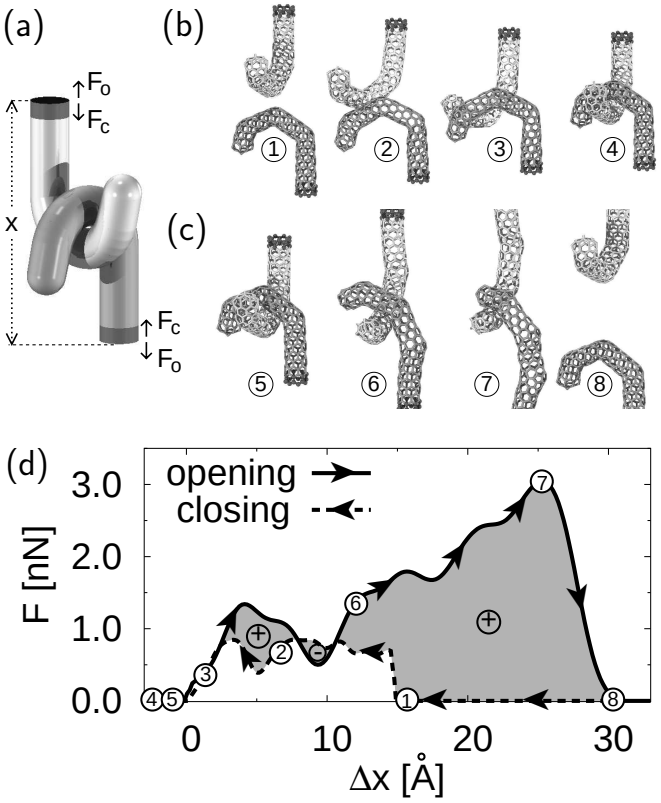

FIG. 2: (a) Schematic drawing of a two-hook assembly, defining the anchor distance x, the direction of the opening force F_o and the closing force F_c. Snap shots of the $(7,0)$ nanohooks during (b) closure and (c) opening of the nanohook assembly. (d) Force acting on the nanohooks during the opening and closure of the assembly as a function of the relative anchor displacement Δx. The labels correspond to structures depicted in (b) and (c). The grey-shaded area, depicting the hysteresis, represents the energy dissipated during an opening-closing cycle.

or a constant velocity in the desired direction.

As illustrated in Fig. 1(a), a set of six pentagon–heptagon pairs causes a permanent deformation of a $(7,0)$ single-wall nanotube to a nanohook [12]. Euler's theorem suggests that a hook deformation due to pentagon-heptagon insertion does not depend on the chiral index of the tube. This is illustrated by comparing the relaxed structures of the $(7,0)$ and the wider $(12,0)$ nanotube in the right panel of Fig. 1(a). Even though substitution of hexagons by pentagon-heptagon pairs in a nanotube is energetically unfavorable, the system is sufficiently flexible to redistribute the strain in the vicinity of the pentagons and heptagons.

To visualize this strain redistribution in the structure, we grey-shaded the spheres representing individual atoms according to their binding energy in Fig. 1(d). We found all the atomic binding energies to be lower than the 7.4 eV value of graphite. The least stable atoms, indicated by the darkest shading in Fig. 1(d), are located in the caps. The atomic arrangement at the hemisphere terminating the $(7,0)$ nanotube is similar to the strained C_{24} fullerene, with atomic binding energies of only $\approx$6.4 eV. The cap structure at the end of the $(12,0)$ nanotube resembles that of the more stable C_{84} fullerene, with atomic binding energies close to 7.1 eV. In general, we expect the occurrence of pentagon-heptagon defects, causing permanently bent structures shown in Figs. 1(b) and (c), primarily at lower synthesis temperatures, where such defects cannot be annealed easily [12, 13].

A pair of mating nanohooks is illustrated schematically in Fig. 2(a), together with the direction of the opening force F_o and the closing force F_c. The nanohooks are to be considered permanently anchored in the surfaces to be connected. The anchor regions are emphasized by the dark color and separated by the distance x. The forces are given by the gradients for the total energy of the nanohook structure with the exception of the rigid edge regions, emphasized by the dark color in Figs. 1(a) and 2(a)-(c). Snap shots of the $(7,0)$ nanohook engagement process are shown in Fig. 2(b). In spite of significant structural deformations during this transition, we found no signs of irreversibility associated with a possible local $sp^2 \rightarrow sp^3$ transition or a permanent structural change, reflecting the resilience of the nanohooks to mechanical deformations.

In our molecular dynamics simulation, we subject the anchor region of the hooks, to a constant velocity $v_c =$ 25 m/s, and monitored the force F_c during the closure process. Comparing results for different velocities, we found the force $F_c(x, v_c)$ to depend only on the relative distance x between the anchor regions at low displacement velocities. Our results indicate that the value of $F_c(x)$, based on molecular dynamics simulations, agrees with static results based on static structure optimization with constrained anchor regions. At velocities $v_c \gtrsim 75$ m/s we observed an increase in $F_c(x, v_c)$ due to the inertia of the nanostructure. For the sake of convenience, we defined $x = x_0 + \Delta x$, where x_0 is the shortest distance between the anchor regions, at which the substructures started interacting. Numerical results for $F_c(\Delta x)$, displayed by the dashed line in Fig. 2(d), indicate that closure of the $(7,0)$ nanohook assembly requires an average force of $< F_c > \approx 0.9$ nN.

The dynamics of the opening process is illustrated by snap shots in Fig. 2(c). As during the closing process, we subjected the anchor regions of the hooks to a low constant velocity $v_o = 25$ m/s and monitored the force F_o during the opening process. The results, given by the solid line in Fig. 2(d), indicate an average opening force of $< F_o > \approx 1.7$ nN, about twice the value of the closing force. The opening force increases as the hook becomes stiffer while stretched, and reaches the maximum value of $F_o \approx 3.0$ nN. In spite of this considerable force, we have not observed any irreversible structural changes in the nanohook assembly, including the least stable ter-

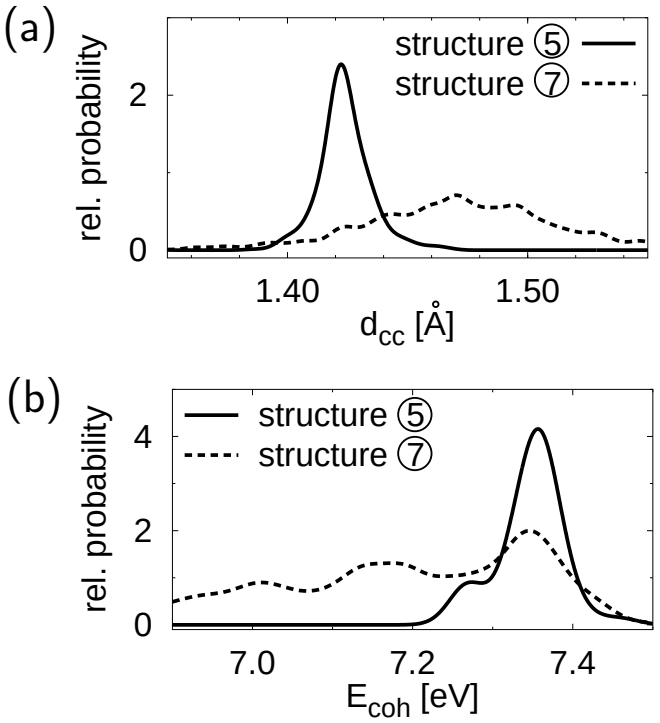

FIG. 3: Distribution of (a) bond lengths and (b) atomic binding energies in the $(7,0)$ nanohook assembly at different stages of the disengagement process. Results for the unstrained structure ⑤ of Fig. 2(c), given by the dotted line, are compared to those for the strained structure ⑦, given by the dotted line.

minating cap. Even in the most strained structure ⑦ in Fig. 2(c), the closest inter-wall distance between the hook substructures was in excess of 2.1 Å, thus preventing a local $sp^2 \rightarrow sp^3$ rebonding [21].

When exploring the suitability of nanohooks for bonding, we assume that the nanohooks are permanently anchored in the substrate by covalent bonds. These bonds are particularly strong for nanohooks grown on diamond, metals and carbides. Uprooting the hook would require a very high force, possibly comparable to the average force of ≈50 nN associated with cleaving the tube axially. The forces needed to open and close the nanovelcro bond are much smaller and will not detach the hook assembly from the anchor points.

To determine, which parts of the nanohook assembly are most prone to damage, we plotted the distribution of bond lengths and atomic binding energies during the opening process in Fig. 3. As seen in Fig. 3(a), most bond lengths are close to the graphite value $d_{CC} = 1.42$ Å in the initial structure ⑤. The corresponding binding energy distribution in Fig. 3(b) shows a large peak near 7.3 eV, reflecting the small strain in the nanotube as compared to a graphene monolayer. Only the cap atoms show a much lower binding energy E_{coh}≈6.4 eV, depicted in Fig. 1(d). In the strained hook structure ⑦, the distortion is accommodated by a large portion of the system, reflecting the ductility of the bond. In the vicinity of the hook, the average bond length increases by ≈0.05 Å and the distribution broadens significantly. This behavior is reflected in the binding energy distribution, which shifts to smaller binding energy values and also broadens considerably. We do not observe new peaks at significantly larger bond lengths or smaller binding energies, which would indicate the onset of a crack. These findings, together with the structural snap shots shown in Figs. 2(b) and (c), confirm that nanovelcro maintains its structural integrity during repeated opening and closing.

Our results in Fig. 2(d) also provide quantitative information about the toughness of the $(7,0)$ nanovelcro bond, defined as the energy needed to open the nanohook assembly. The calculated toughness of ≈30 eV is very high, almost twice the energy investment of 15.4 eV to cleave a perfect $(7,0)$ nanotube. The simple reason for this unexpected result is that an average opening force $< F_o >$ ≈1.7 nN, acting over a large distance of 30 Å, performs more work than the much higher force of ≈50 nN, which cleaves axial bonds across a distance of 0.5 Å. Upon opening, the energy stored in the strained hook structure is deposited into the internal degrees of freedom, heating up the nanostructure locally up to near $1,000$ K. This energy is efficiently carried away due to the excellent thermal conductivity of carbon nanotubes [22], thus preventing irreversible structural changes.

Next, we define the stability of the nanovelcro bond as the energy to close and reopen the nanohook assembly, given by $\Delta E_b = \int_{-\infty}^{\infty} (F_o(x) - F_c(x))\, dx$. We find a large value of ΔE_b≈24 eV for the stability of the $(7,0)$ nanohook system, corresponding to the shaded area in Fig. 2(d). The relatively small difference between the toughness and the stability of the bond is due to the low amount of energy required to close the hook, given by the area under the dotted line.

The usefulness of nanovelcro for permanent bonding becomes obvious especially when considering two flat solid surfaces covered by an array of nanohooks. In view of the small nanohook cross-section, we may find up to one nanohook per nm^2, corresponding to an ideal coverage of 10^{18} nanohooks per m^2. Thus, detachement of nanovelcro bonded areas should require an energy investment of $\lesssim$5 J/m^2. This is significantly more than the energy to cleave most crystals, which is twice their surface energy, and is responsible for the unusual toughness of the nanovelcro bond. In view of the large force required to open a nanohook assembly, the ultimate strength of nanovelcro should approach 3 GPa, more than in most solids. Under tensile load, we expect the solids to break first, while the nanovelcro bonds remain engaged.

We found that the bonding ability deteriorates with increasing nanotube diameter. In the wider nanohook based on the $(12,0)$ nanotube, we found that the resilience of the system is reduced by its tendency to col-

lapse upon bending. This particular deficit can be compensated by using multi-wall nanotubes or peapods [23] instead of single-wall systems.

As we did not observe any $sp^2 \rightarrow sp^3$ rebonding during our simulation, we compared our total energies to calculations based on the Tersoff potential [20]. Since this bond-order potential considers nearest-neighbor bonds only, the optimized hook structures were slightly wider and the work associated with their opening and closing turned out to be about 10% lower than in the results presented above.

It is essential to notice that the the crucial feature of the nanovelcro bond is not the shape of the deformed nanotubes, but rather the area under the force-displacement hysteresis curve in Fig. 2(d). Other structures, including coils [24], can be combined with hooks and other deformed tubes for efficient bonding. We expect the bonded area to show good electrical and thermal conductivity, reflecting the intrinsic properties of nanotubes. Conductivity measurements can also be used to monitor the local bonding in real time. A uniform surface coverage by nanohooks can be achieved using Chemical Vapor Deposition of hydrocarbons on catalyst-covered surfaces [25], as seen in Fig. 1(c). The requirement of a low growth temperature for the formation of hook structures also extends the range of substrates, on which nanovelcro can be grown. The ability of hooks to open and close reversibly results in a unique self-repairing capability. This is of particular interest when bonding solids with different thermal expansion, such as applying a diamond coating to metals, since self-repair should prevent delamination in case of large temperature fluctuations.

In conclusion, we combined total energy and molecular dynamics calculations to explore the suitability of nanotube-based hooks for bonding. Hooks, coils, and similar structures form upon inserting pentagon-heptagon pairs in the honeycomb structure of straight carbon nanotubes. We postulated that surfaces covered with an array of hooks, which are covalently anchored in the substrate, can be pressed together and form permanent bonds as a nanoscale counterpart of velcro fasteners. Our results indicate that a large force of 3.0 nN is required to disengage two hooks based on a $(7,0)$ carbon nanotube. Performing simulations for $(7,0)$ and $(12,0)$ systems, we found nanohooks to be generally resilient and to keep their structural integrity during the opening and closing process. In view of the high tensile strength of individual nanotubes and the stability of nanotube-substrate bonds, arrays of hooks may connect solids ranging from metals to carbides and diamond with a tough, heat resistant bond. This bonding scheme shows a capability for self-repair that may prevent delamination caused by differential thermal expansion. Nanovelcro bears promise as a micro-fastening system for the next generation of nano-robots and nanometer-scale mechanical and electronic components.

We acknowledge useful discussions about nanovelcro with Mina Yoon and Richard Enbody. We thank Sumio Iijima and Jean-Christophe Gabriel for drawing our attention to their synthesis of nanohook structures. This work was partly supported by NSF-NIRT grant DMR-0103587.

* Present address: Nanomix, Inc., 5980 Horton Street, Suite 600, Emeryville, California 94608
† E-mail: tomanek@msu.edu

[1] Sumio Iijima, Nature (London) **354**, 56 (1991).
[2] R. Saito, G. Dresselhaus, and M.S. Dresselhaus, *Physical Properties of Carbon Nanotubes* (Imperial College Press, 1998).
[3] G. Overney, W. Zhong, and D. Tománek, Z. Phys. D **27**, 93 (1993).
[4] M.M.J. Treacy, T.W. Ebbesen, and J.M. Gibson, Nature (London) **381**, 678 (1996).
[5] M. R. Falvo *et al.*, Nature (London) **389**, 582 (1997).
[6] B. I. Yakobson, C.J. Brabec, and J. Bernholc, Phys. Rev. Lett. **76**, 2511 (1996).
[7] Jian Ping Lu, Phys. Rev. Lett. **79**, 1297 (1997).
[8] W. N. Reynolds, *Physical Poperties of Graphite* (Elsevier, Amsterdam 1968).
[9] S. Iijima and T. Ichihashi, Nature (London) **363**, 603 (1993).
[10] D.S. Bethune *et al.*, Nature (London) **363**, 605 (1993).
[11] R. Saito, G. Dresselhaus, and M. S. Dresselhaus, Phys. Rev. B **53**, 2044 (1996).
[12] S. Iijima, MRS Bulletin **19**, No. 11, 43 (1994).
[13] Jean-Christophe Gabriel (private communication).
[14] B.I. Dunlap, Phys. Rev. BR **46**, 1933 (1992); J. C. Charlier, T. W. Ebbesen, P. Lambin, Phys. Rev. B **53**, 11108 (1996).
[15] *"Micro-Fastening System and Method of Manufacture".* U.S. Patent Application of D. Tománek, Richard J. Enbody, and Young-Kyun Kwon, filed February 12, 1998.
[16] S. Berber, Y.-K. Kwon, and D. Tománek, Phys. Rev. Lett. **88**, 185502 (2002).
[17] Young-Kyun Kwon *et al.*, Phys. Rev. Lett. **79**, 2065 (1997).
[18] Young-Kyun Kwon, David Tománek, and Sumio Iijima, Phys. Rev. Lett. **82**, 1470 (1999).
[19] S.G. Kim and D. Tománek, Phys. Rev. Lett. **72**, 2418 (1994).
[20] J. Tersoff, Phys. Rev. Lett. **61**, 2879 (1988).
[21] S. Fahy, S.G. Louie, and M.L. Cohen, Phys. Rev. B **34**, 1191 (1986).
[22] Savas Berber, Young-Kyun Kwon, and David Tománek, Phys. Rev. Lett. **84**, 4613 (2000).
[23] B.W. Smith, M. Monthioux, and D.E. Luzzi, Nature **396**, 323 (1998).
[24] P. Simonis *et al.*, in *Science and Application of Nanotubes*, edited by D. Tománek and R. J. Enbody (Kluwer Academic, New York, 2000), p. 83.
[25] Z. F. Ren *et al.*, Science **282**, 1105 (1999).

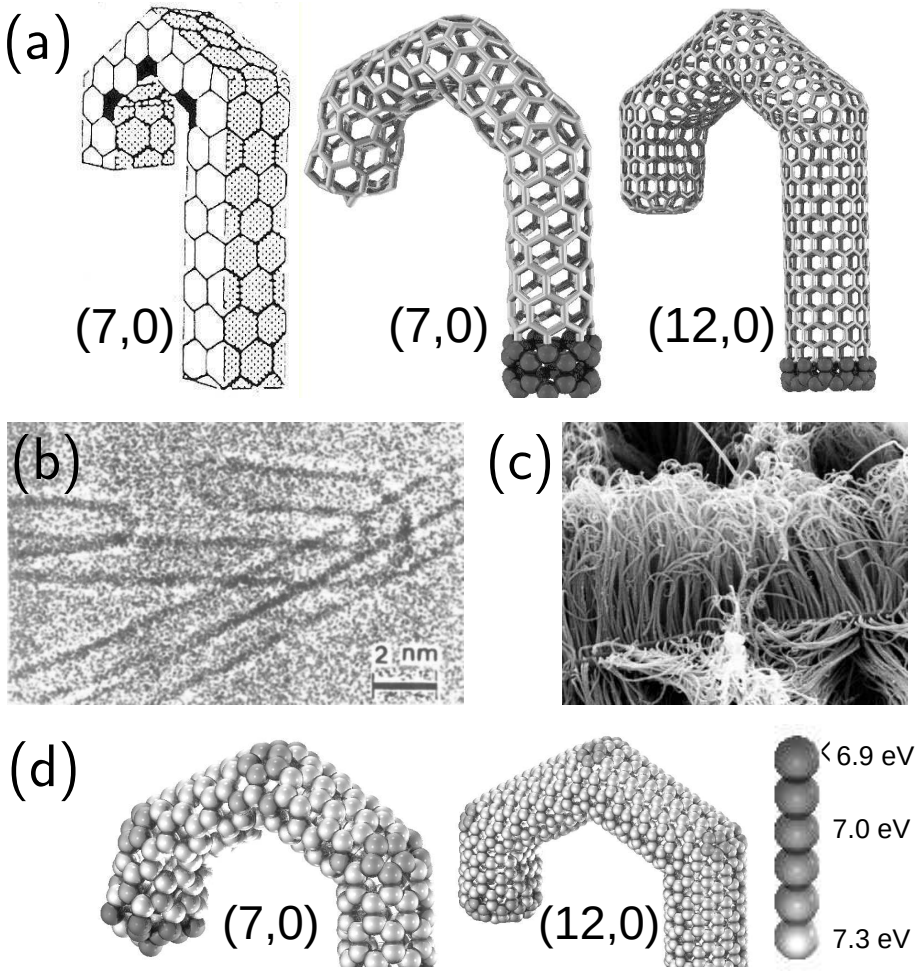

Figure 1

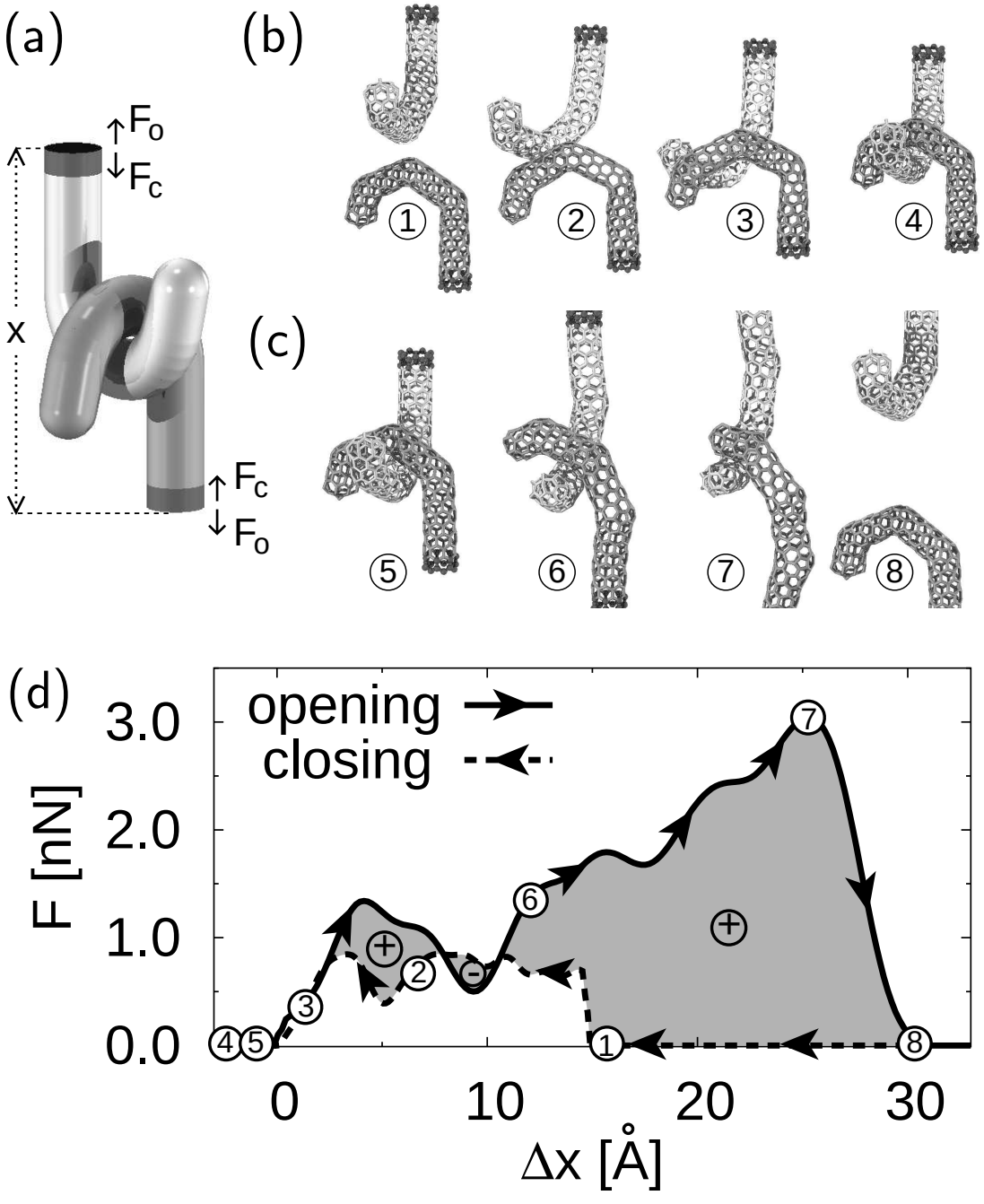
(a)
(b)
(c)
(d)
F_o
F_c
x
F_c
F_o
①
②
③
④
⑤
⑥
⑦
⑧
opening
closing
F [nN]
3.0
2.0
1.0
0.0
0
10
20
30
Δx [Å]

Figure 2

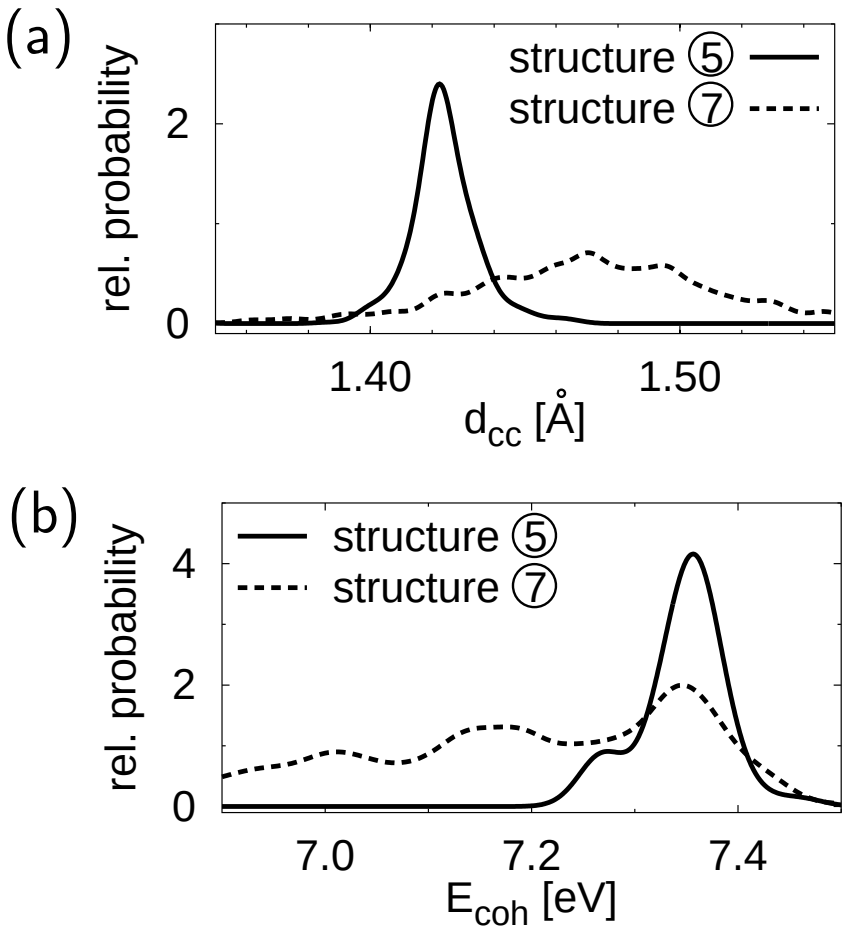
(a)
rel. probability
structure ⑤
structure ⑦
2
0
1.40
1.50
d_{cc} [Å]
(b)
rel. probability
structure ⑤
structure ⑦
4
2
0
7.0
7.2
7.4
E_{coh} [eV]

Figure 3